

## Dansgaard-Oeschger cycles: Interactions between ocean and sea ice intrinsic to the Nordic seas

Trond M. Dokken,<sup>1,2</sup> Kerim H. Nisancioglu,<sup>1,2,3</sup> Camille Li,<sup>2,4</sup> David S. Battisti,<sup>2,5</sup> and Catherine Kissel<sup>6</sup>

Received 20 May 2013; revised 16 July 2013; accepted 16 July 2013; published 12 September 2013.

[1] Dansgaard-Oeschger (D-O) cycles are the most dramatic, frequent, and wide-reaching abrupt climate changes in the geologic record. On Greenland, D-O cycles are characterized by an abrupt warming of  $10 \pm 5^\circ\text{C}$  from a cold stadial to a warm interstadial phase, followed by gradual cooling before a rapid return to stadial conditions. The mechanisms responsible for these millennial cycles are not fully understood but are widely thought to involve abrupt changes in Atlantic Meridional Overturning Circulation due to freshwater perturbations. Here we present a new, high-resolution multiproxy marine sediment core monitoring changes in the warm Atlantic inflow to the Nordic seas as well as in local sea ice cover and influx of ice-rafted debris. In contrast to previous studies, the freshwater input is found to be coincident with warm interstadials on Greenland and has a Fennoscandian rather than Laurentide source. Furthermore, the data suggest a different thermohaline structure for the Nordic seas during cold stadials in which relatively warm Atlantic water circulates beneath a fresh surface layer and the presence of sea ice is inferred from benthic oxygen isotopes. This implies a delicate balance between the warm subsurface Atlantic water and fresh surface layer, with the possibility of abrupt changes in sea ice cover, and suggests a novel mechanism for the abrupt D-O events observed in Greenland ice cores.

**Citation:** Dokken, T. M., K. H. Nisancioglu, C. Li, D. S. Battisti, and C. Kissel (2013), Dansgaard-Oeschger cycles: Interactions between ocean and sea ice intrinsic to the Nordic seas, *Paleoceanography*, 28, 491–502, doi:10.1002/palo.20042.

### 1. Introduction

[2] There is a wealth of proxy data showing that the climate system underwent large, abrupt changes throughout the last ice age. Among these are about one score large, abrupt climate changes known as Dansgaard-Oeschger events that occurred every 1–2 kyr. These events were first identified in ice cores taken from the summit of Greenland [Dansgaard *et al.*, 1993; Bond *et al.*, 1993] and are characterized by an abrupt warming of  $10 \pm 5^\circ\text{C}$  in annual average temperature [Severinghaus and Brook, 1999; Lang *et al.*, 1999; NGRIP, 2004; Landais *et al.*, 2004; Huber *et al.*, 2006]. Subsequent observational studies demonstrated that

the D-O events represent a near-hemispheric scale climate shift (see, e.g., Voelker [2002] and Rahmstorf [2002] for an overview). Warming in Greenland is coincident with warmer, wetter conditions in Europe [Genty *et al.*, 2003], an enhanced summer monsoon in the northwest Indian Ocean [Schulz *et al.*, 1998; Pausata *et al.*, 2011], a northward shift of precipitation belts in the Cariaco Basin [Peterson *et al.*, 2000], aridity in the southwestern United States [Wagner *et al.*, 2010], and changes in ocean ventilation off the shore of Santa Barbara, California [Hendy *et al.*, 2002]. Each abrupt warming shares a qualitatively similar temperature evolution: about 1000 years of relatively stable cold conditions, terminated by an abrupt (less than 10 years) jump to much warmer conditions that persist for 200–400 years, followed by a more gradual transition (~50 to 200 years) back to the cold conditions that precede the warming event. This sequence of climate changes is often referred to as a D-O cycle.

[3] The leading hypothesis for D-O cycles attributes them to an oscillation of the Atlantic Meridional Overturning Circulation (AMOC) [Broecker *et al.*, 1985], with “on” and “off” (or “weak”) modes of the AMOC [Stommel, 1961; Manabe and Stouffer, 1988] producing warm interstadials and cold stadials, respectively, through changes in the meridional ocean heat transport. Indeed, interstadial and stadial conditions on the Greenland summit are associated with markedly different water mass properties (temperature and salinity) in the North Atlantic [Curry and Oppo, 1997] and Nordic seas [Dokken and Jansen, 1999]. Transitions between the two phases are thought to arise from changes in the freshwater

<sup>1</sup>UNI Research AS, Bergen, Norway.

<sup>2</sup>Bjerknes Centre for Climate Research, Bergen, Norway.

<sup>3</sup>Department of Earth Science, University of Bergen, Bergen, Norway.

<sup>4</sup>Geophysical Institute, University of Bergen, Bergen, Norway.

<sup>5</sup>Department of Atmospheric Sciences, University of Washington, Seattle, Washington, USA.

<sup>6</sup>Laboratoire des Sciences du Climat et de l'Environnement, CEA/CNRS/UVSQ, Gif-sur-Yvette, France.

Corresponding author: K. H. Nisancioglu, Department of Earth Science, University of Bergen, Allegaten 70, 5007 Bergen, Norway. (kerim@bjerknes.uib.no)

©2013. The Authors.

This is an open access article under the terms of the Creative Commons Attribution-NonCommercial-NoDerivs License, which permits use and distribution in any medium, provided the original work is properly cited, the use is non-commercial and no modifications or adaptations are made. 0883-8305/13/10.1002/palo.20042

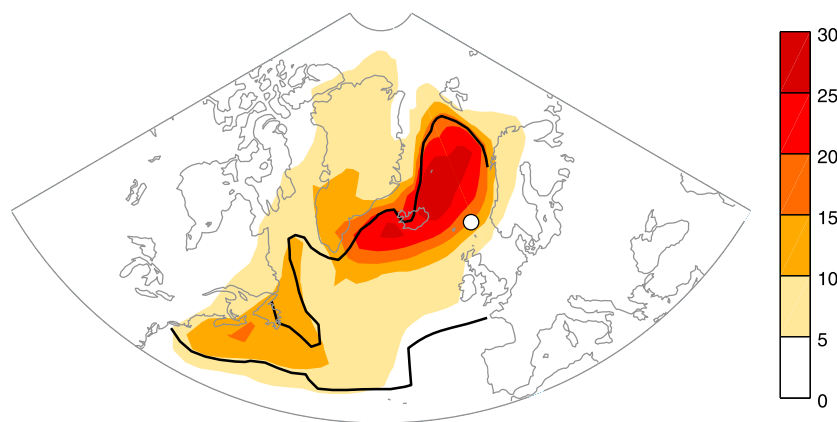


**Figure 1.** Surface air temperature response during the extended winter season (December–April) to changes in Nordic seas ice cover (figure redrawn from simulations in *Li et al.* [2010]). Black contours indicate maximum (March) ice extent in the two scenarios. The white dot is the location of our core MD992284.

budget of the North Atlantic [*Broecker et al.*, 1990]. In particular, *Birchfield and Broecker* [1990] proposed that the continental ice sheets covering North America and Eurasia were the most likely sources for the freshwater [see also *Petersen et al.*, 2013]. Abrupt events later during the deglaciation may have seen a contribution from Antarctica as well [*Clark et al.* 2001], but it is not clear that the underlying mechanisms for these events are the same as for the D-O events occurring prior to the Last Glacial Maximum (21 kyr).

[4] A number of studies with climate models of intermediate complexity (EMICs) have produced two quasi-stable phases in the AMOC by imposing ad hoc cyclic freshwater forcing [*Marotzke and Willebrand*, 1991; *Ganopolski and Rahmstorf*, 2001; *Knutti et al.*, 2004]. Although these models simulate a temperature evolution on the Greenland summit that is qualitatively similar to observations, the changes in the simulated local and far-field atmospheric response are small compared to observations. Similar experiments with state-of-the-art climate models produce local and far-field responses that are in better agreement with the proxy data [e.g., *Vellinga and Wood*, 2002]. However, these models require unrealistically large freshwater perturbations, and on Greenland, the simulated stadial to interstadial transitions are not as abrupt as observed. In both cases, the prescribed external forcing is ad hoc and yet is entirely responsible for the existence and the longevity of the two phases (i.e., the cold phase exists as long as the freshwater forcing is applied).

[5] Despite the unresolved questions surrounding D-O cycles, there has been progress. The direct, causal agent for the abrupt climate changes associated with D-O warming events is thought to be abrupt reductions in North Atlantic sea ice extent [*Broecker*, 2000; *Gildor and Tziperman*, 2003; *Masson-Delmotte et al.*, 2005; *Jouzel et al.*, 2005]. Studies using atmospheric general circulation models (AGCMs) show that the local precipitation and temperature shifts (inferred from oxygen isotopes and accumulation changes) on the Greenland summit associated with a typical D-O event are consistent with the response of the atmosphere to a reduction in winter sea ice extent, in particular in the Nordic seas region (e.g., Figure 1) [see also *Renssen and Isarin*, 2001; *Li et al.*, 2005, 2010]. Away from the North Atlantic, the northward shift of tropical precipitation belts

associated with D-O warming events mirrors the southward shift simulated by coupled climate models in response to freshwater hosing and expansion of sea ice [*Vellinga and Wood*, 2002; *Otto-Bliesner and Brady*, 2010; *Lewis et al.*, 2010] and by AGCMs coupled to slab ocean models in response to a prescribed expansion of North Atlantic sea ice [*Chiang et al.*, 2003], thus supporting the existence of a robust link between North Atlantic sea ice cover and far-field climate.

[6] More recently, a number of studies have shown that cold stadial conditions are associated with subsurface and intermediate depth warming in the North Atlantic [*Rasmussen and Thomsen*, 2004; *Marcott et al.*, 2011]. This subsurface warming may have bearing on many aspects of D-O cycles, from the abruptness of the warming (stadial-to-interstadial) transitions [*Mignot et al.*, 2007] to the possibility of ice shelf collapses during D-O cycles [*Álvarez-Solas et al.*, 2011; *Marcott et al.*, 2011; *Petersen et al.*, 2013].

[7] In this study, we focus on the subsurface warming rather than ice rafting to build physical arguments for the mechanisms behind D-O cycles. Changes in sea ice and subsurface ocean temperatures during D-O transitions are linked to each other by the ocean circulation and to changes in Greenland by the atmospheric circulation. To elucidate these links requires marine records that (i) are situated in key regions of the North Atlantic, (ii) are representative of conditions through the depth of the water column, and (iii) can be compared to records of atmospheric conditions (as measured from the Greenland summit) with a high degree of certainty in terms of timing. In addition, because of the abruptness of the transitions (on the order of decades or less), the marine records must be of exceptionally high resolution.

[8] Here we present new data from a Nordic seas core that meet these criteria. The core site is strategically located in the Atlantic inflow to the Nordic seas, where extremely high sedimentation rates allow for decadal-scale resolution of both surface and deepwater proxies. In addition to an age model based on calibrated carbon-14 ages and magnetic properties, ash layers provide an independent chronological framework to synchronize signals in the marine core with signals in an ice core from the summit of Greenland.

[9] The new marine proxy data reveal systematic changes in the hydrography of the Nordic seas as Greenland swings from stadial (cold) to interstadial (warm) conditions and back

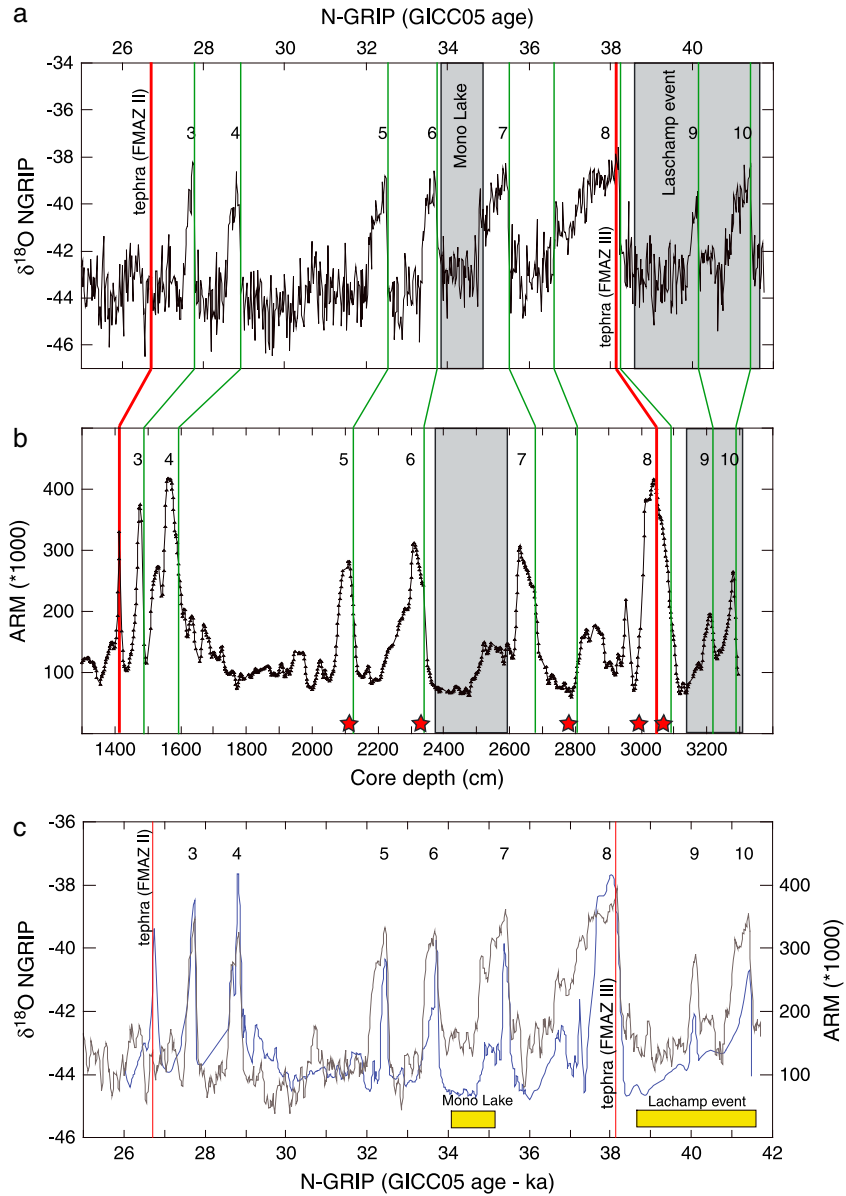


**Figure 2.** (a)  $\delta^{18}\text{O}$  of NGRIP plotted versus time (in kyr). (b) Measured low-field magnetic susceptibility, anhysteretic remanent magnetization (ARM) (log scale/unit  $10^{-6}$  A/m) in MD992284 plotted versus depth. Red stars indicate the stratigraphical level (depths) from where AMS  $^{14}\text{C}$  ages are measured (see also Table 1). (c) NGRIP  $\delta^{18}\text{O}$  (black line) and ARM (blue line) record from MD992284 after converting the MD992284 age to the NGRIP age (b2k). Green vertical lines indicate tuning points for the (numbered) onset of interstadials in the ice core and marine records. Red vertical lines connect identical ash layers (FMAZ III and FMAZ II) in NGRIP and MD992284 as described in the text and in Table 1.

through several D-O cycles, with details of the transitions better resolved than in any previously studied core. The interstadial phase in the Nordic seas is shown to resemble current conditions, while the stadial phase has greatly enhanced sea ice coverage (as inferred from benthic oxygen isotopes) and a hydrographic structure similar to that in the Arctic Ocean today. The variations recorded by the marine proxies near the transitions are used to determine the possible mechanisms that cause the North Atlantic climate system to jump abruptly from stadials to interstadials and to transition slowly back from interstadials to stadials. In a departure from most existing hypotheses for the D-O cycles, the conceptual model

presented here does not require freshwater fluxes from ice sheets to enter the ocean at specific times during the D-O cycle [e.g., *Birchfield and Broecker, 1990; Petersen et al., 2013*]. Rather, it relies on ocean-sea ice interactions internal to the Nordic seas to trigger stadial-interstadial transitions.

[10] The paper proceeds as follows. Section 2 contains a description of the marine sediment core, analysis methods, the construction of the age model for the core, and the construction of a common chronology with an ice core from the summit of Greenland. Section 3 describes the cold stadial and warm interstadial climate of the Nordic seas as seen in the marine sediment data. Section 4 analyzes the relevance

of the new proxy data for the D-O cycles as observed on Greenland and, in particular, the mechanisms behind the abrupt transitions. Section 5 presents a summary of the results and a discussion of the implications.

## 2. Materials and Methods

[11] Core MD992284 was collected in the Nordic seas during the MD114/IMAGES V cruise aboard R/V *Marion Dufresne* (IPEV) at a water depth of 1500 m on the northeastern flank of the Faeroe-Shetland channel. The core is strategically located in the Atlantic inflow to the Nordic seas and has an exceptionally high sedimentation rate, allowing for decadal-scale resolution of both surface and deep water proxies. The unique, high-resolution marine core with a well constrained age model (Figure 2) shows evidence for systematic differences in the Nordic seas during Greenland interstadials versus Greenland stadials. These new data are used to characterize the important hydrographic features of the Nordic seas in each of these two phases of the D-O cycle as well as the transition between the phases.

[12] Figure 2a shows a segment of the North Greenland Ice Core Project (NGRIP) ice core from Greenland [NGRIP, 2004] during late Marine Isotope Stage 3 (MIS3) containing several typical D-O cycles. To compare the marine record to the ice core record, we have constructed an age model by matching rapid transitions in MD992284 to NGRIP using the Greenland Ice Core Chronology 2005 (GICC05) [Svensson *et al.*, 2006] and ash layers found in both cores. The common chronology allows the Nordic seas data to be linked directly to Greenland ice core signals.

### 2.1. Age Model for Marine Sediment Core

[13] Age models based on the ice core and calibrated  $^{14}\text{C}$  dates can be used to estimate “true ages” for the marine core but will be subject to errors due to missing or misinterpreted ice layers, uncertainty in reservoir ages, and uncertainty in sedimentation rates. Our approach here is thus not to rely on true ages, but rather on a stratigraphic tuning of the marine record to the ice core record. We use the high-frequency variations in measured anhysteretic remanent magnetization (ARM) during Marine Isotope Stage 3 (MIS3) in the marine core (Figure 2b). The fast oscillations in magnetic properties during MIS3 in the North Atlantic/Nordic seas have been shown to be in phase with changes in  $\delta^{18}\text{O}$  of Greenland ice cores [Kissel *et al.*, 1999]. We use the ARM record for tuning only, with no further subsequent paleoproxy interpretation of this parameter. The tuning has been performed using the tuning points as indicated in Figure 2 and the software package AnalySeries 2.0 [Paillard *et al.*, 1996].

[14] A final step in the synchronization between the ice core and the marine core is done with tephra layers. Two ash zones identified in the marine record have also been identified in the NGRIP ice core [Svensson *et al.*, 2008], the Fugloyarbanki Tephra (FMAZII) [Davies *et al.*, 2008] and Fareo Marine Ash Zone III (FMAZIII) [Wastegård *et al.*, 2006]. These ashes allow for a direct, independent comparison between the marine and ice core records. Our chronology places the ash layer FMAZIII less than 100 years after the onset of interstadial 8 in NGRIP (see Figure 2) and thus provides a verification of the initial tuning of the ARM record in MD992284 to the  $\delta^{18}\text{O}$  record in NGRIP. These two ash

layers are also used as tuning points in the final age model. The final age model gives the best possible synchronization of the marine record to the NGRIP ice core record [NGRIP, 2004], making it possible to determine the relative timing of observed changes in the marine proxies compared to temperature changes on Greenland.

[15] The final tuned age model presented for MIS3 (Figure 3) only uses the ages given by the tuning to NGRIP and the ash layers. As an independent check, we note that the new age model for the marine sediment core is consistent with calibrated  $^{14}\text{C}$  dates (Table 1). These are calculated using the calibration software CALIB 6.0 [Stuiver and Reimer, 1993] and an ocean reservoir age of 400 years, applying the “Marine09” calibration curve [Hughen *et al.*, 2004] for ages younger than 25 kyr B.P. ( $^{14}\text{C}$  age, kilo years before present) and the “Fairbanks0107” calibration curve for anisotropy of magnetic susceptibility (AMS)  $^{14}\text{C}$  samples of ages older than 25 kyr B.P. [Fairbanks *et al.*, 2005]. Offsets of at least a few thousand years from the true age are expected due to the relatively large error in  $^{14}\text{C}$  measurements in the interval of 30–40 kyr B.P., as well as errors in transformation from  $^{14}\text{C}$  ages to calibrated ages. Additional error is introduced by the assumption that sedimentation rates are constant between the dated levels.

### 2.2. Near-Surface Ocean Temperature Estimates

[16] For the planktonic foraminifera, raw census data of the planktonic assemblages were analyzed and the transfer function technique (maximum likelihood (ML)) was used to calculate near-surface temperature. The ML method operates with a statistical error close to  $\pm 1^\circ\text{C}$  and is found to give the least autocorrelation compared to other statistical methods [Telford and Birks, 2005].

### 2.3. Transforming the $\delta^{18}\text{O}$ Into a Measure of Seawater Isotopic Composition

[17] The ratio of oxygen-18 to oxygen-16 as they are incorporated into foraminiferal calcite ( $\delta^{18}\text{O}_{\text{calcite}}$ ) is dependent on both seawater  $\delta^{18}\text{O}$  (expressed as per mil deviations from Vienna Standard Mean Ocean Water (SMOW)) and calcification temperature. Foraminifera-based SST estimates provide an independent estimate of the calcification temperature and therefore the temperature effects on calcite  $\delta^{18}\text{O}$ .

[18] The temperature to  $\delta^{18}\text{O}$  calibration used is based on Kim and O’Neil [1997]:

$$T = 16.1 - 4.64 (\delta^{18}\text{O}_{\text{calcite}} - \delta^{18}\text{O}_{\text{SMOW}}) + 0.09 (\delta^{18}\text{O}_{\text{calcite}} - \delta^{18}\text{O}_{\text{SMOW}})^2$$

[19] Knowing the calcification temperature (T) from the foram transfer function and the measured  $\delta^{18}\text{O}_{\text{calcite}}$ , we can extract the isotopic composition of the ambient sea water ( $\delta^{18}\text{O}_{\text{SMOW}}$ ). The relationship between salinity and  $\delta^{18}\text{O}_{\text{SMOW}}$  in the ocean depends on the spatial variation of  $\delta^{18}\text{O}$  associated with the fresh water flux to the ocean, the amount of seawater trapped in ice caps, as well as ocean circulation [Bigg and Rohling, 2000].

[20] Before translating glacial  $\delta^{18}\text{O}$  data into a measure of  $\delta^{18}\text{O}_{\text{SMOW}}$ , the effect of global ice volume must be accounted for. Fractionation processes of oxygen isotopes when water

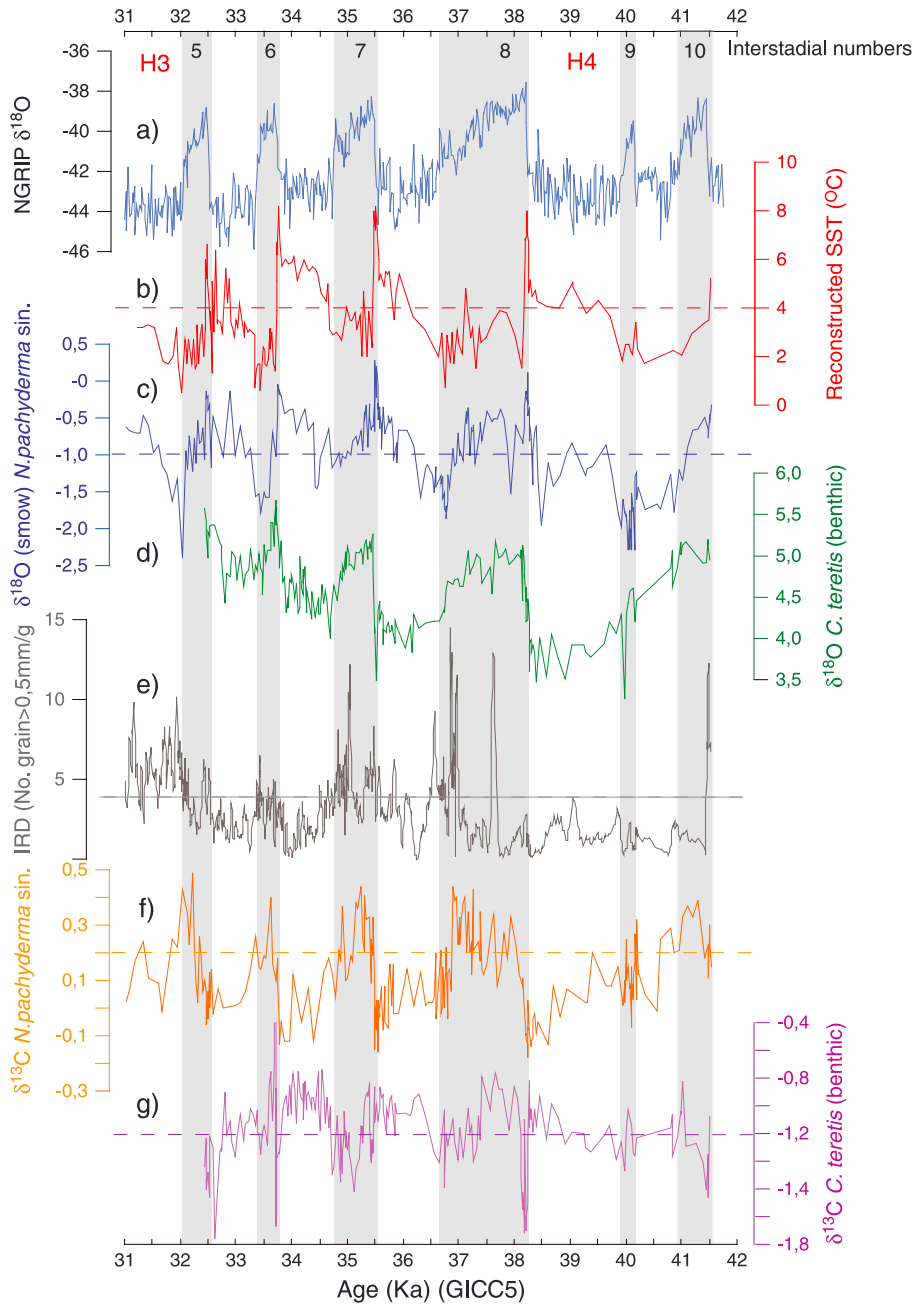


**Figure 3.** Down core data sets from NGRIP and MD992284 covering the period 41 to 31 ka plotted on the GICC05 (b2k) time scale. (a) NGRIP  $\delta^{18}\text{O}$  (proxy for Greenland temperature), (b) MD992284 reconstructed temperature based on planktonic foram assemblages, (c) MD992284 near-surface  $\delta^{18}\text{O}_{\text{SMOW}}$ , (d) MD992284 benthic  $\delta^{18}\text{O}$ , (e) MD992284 flux-corrected ice-rafted debris (IRD), (f) MD992284 near-surface  $\delta^{13}\text{C}$ , and (g) MD992284 benthic  $\delta^{13}\text{C}$ . Interstadial periods are indicated by grey shading. The near-surface  $\delta^{18}\text{O}_{\text{SMOW}}$  is determined from the *Kim and O'Neil* [1997] calibration curve using the  $\delta^{18}\text{O}$  of *N. pachyderma* sin. and the temperature obtained using transfer functions (see section 2). The near-surface  $\delta^{13}\text{C}$  is measured on *N. pachyderma* sin. and the benthic  $\delta^{18}\text{O}$  and  $\delta^{13}\text{C}$  are measured on *Cassidulina teretis*.

freezes into ice produce an ocean-wide  $\delta^{18}\text{O}$  shift of about 0.1‰ per 10 m of sea level stored in continental ice sheets [Fairbanks, 1989]. A review of recent advances in the estimates of sea level history during MIS3 is given by Siddall et al. [2008]. The estimated sea level changes during MIS3 vary in amplitude and timing between the different reconstructions. In our study, we use the sea level reconstruction of

Waelbroeck et al. [2002], which fits well with available coral-based estimates for MIS3, to remove the effects of changing ice volume on the  $\delta^{18}\text{O}$  of ocean water. Note that the sea level correction is only applied to the planktonic  $\delta^{18}\text{O}$  data. In the benthic record, the gradual decrease in sea level as well as a general cooling toward the Last Glacial Maximum is seen as a long term trend in the  $\delta^{18}\text{O}$  (Figure 3d).

**Table 1.** Radiocarbon-Dated Intervals Used as a First Approximation to Create the Age Model<sup>a</sup>

Laboratory Reference and Ash Identity	Mean Depth (cm)	<sup>14</sup> C Age, Uncorrected (yr B.P.)	Error, 1 $\sigma$ (yr)	Calibrated Ages - Intercept (kyr)	Max. 1 $\sigma$ Calibrated Age (yr B.P.)	Min. 1 $\sigma$ Calibrated Age (yr B.P.)
TUa-3310	1,100.5	21,975	160	24.64	25,018	24,270
FMAZ II	1,407.5			26.69 (b2k)		
POZ-29522	2,106.5	29,100	240	34.06	33,770	34,350
POZ-29523	2,324.5	29,900	600	34.87	34,260	35,480
POZ-17620	2,775.5	29,920	240	35.5	36,000	35,000
POZ-17621	2,996.5	32,500	300	37.5	37,800	37,100
FMAZ III	3,040.5			38.07 (b2k)		
POZ-29524	3,075.5	34,600	700	39.53	38,830	40,230

<sup>a</sup>All AMS <sup>14</sup>C ages are measured on *N. pachyderma* sin. Also shown in the table are two identified ash layers. The ages given for Fugloyarbanki Tephra (FMAZII) and Faroe Marine Ash Zone III (FMAZIII) are from Svensson *et al.* [2008]. The ash ages are referred to in b2k (before year A.D. 2000). Samples with laboratory reference “TUa-” are measured at the Uppsala Accelerator in Sweden, but the samples have been prepared at the radiocarbon laboratory in Trondheim, Norway. Samples labeled “POZ-” are prepared and measured in the radiocarbon laboratory in Poznan, Poland.

#### 2.4. Interstadial and Stadial Phases of a D-O Cycle

[21] Positioned in the path of inflowing warm Atlantic water to the Nordic seas and close to the routing of freshwater from the Fennoscandian ice sheet, our marine sediment core is ideally suited to better understand the changes to the hydrography and sea ice cover of the Nordic seas during MIS3. The use of an accurate age chronology constrained by common tephra layers located at key transitions in the marine and ice cores makes it possible to compare individual stadial and interstadial periods between the two climate archives. Here we will describe the warm and cold phases of D-O cycles as seen in the new Nordic seas sediment core data and compare them to the Greenland ice core record before examining the transitions in section 4.

#### 2.5. The Nordic Seas During Greenland Stadials

[22] Foraminiferal assemblages used to reconstruct near-surface ocean temperature show that water masses at the core site in the Nordic seas are  $\sim 2^\circ\text{C}$  warmer during cold Greenland stadials than during warm interstadials (Figure 3b). Further, there is a warm overshoot at the onset of each interstadial. Despite difficulties in acquiring reliable low-temperature reconstructions in polar and Arctic water masses [e.g., Pflaumann *et al.*, 2003; Meland *et al.*, 2005], the estimated higher temperatures during stadials compared to interstadials are a robust result. This is based on higher percentages of “Atlantic species” associated with relatively warm conditions (such as *Globigerina bulloides*, *Neogloboquadrina pachyderma* (dextral), and *Turborotalita quinqueloba*) and accounting for  $\sim 20$ – $30\%$  of the total planktonic assemblage during stadials. Interstadials are instead dominated by cold water (Arctic) species such as *Neogloboquadrina pachyderma* (sinistral), which account for nearly 100% of the total planktonic assemblage.

[23] Planktonic foraminifera are known to change their depth habitat in Arctic environments to avoid the low-salinity surface, which is separated from the subsurface warm Atlantic layer by a halocline (strong vertical salinity gradient). This results in different depth distributions of foraminifera under different hydrographic conditions [Carstens *et al.*, 1997]. Therefore, a reasonable interpretation of these data is that, during cold stadials in the Nordic seas, the planktonic assemblages are located below the fresh surface layer and thus record the relatively warm temperatures just below the halocline (Figure 4, left). At these depths, the foraminifera

are in contact with relatively warm Atlantic water that is isolated from the atmosphere by the halocline and sea ice cover, both of which are features of the stadial phase of the D-O cycle. Note that at the end of each stadial phase, there is a warm overshoot that provides a clue to understanding the stadial-to-interstadial transition (discussed in section 4).

[24] Combining stable isotope ( $\delta^{18}\text{O}_{\text{calcite}}$ ) measurements on the planktonic foraminifera *N. pachyderma* sin. with the ocean temperature reconstruction produces an estimate of the isotopic composition of sea water ( $\delta^{18}\text{O}_{\text{SMOW}}$ ).  $\delta^{18}\text{O}_{\text{SMOW}}$  is partly related to salinity, but it also reflects spatial shifts in water masses. The isotopic composition of polar water may be different compared to water of subtropical origin, but because the planktonic foraminifera prefer to stay within the warm Atlantic layer, we do not expect that the mean  $\delta^{18}\text{O}_{\text{SMOW}}$  (salinity) at the core site will be substantially different during stadials compared to interstadials. Indeed, we see in Figure 3c that there is no systematic difference in the mean  $\delta^{18}\text{O}_{\text{SMOW}}$  during stadial and interstadial periods. The common near-surface temperature spikes at

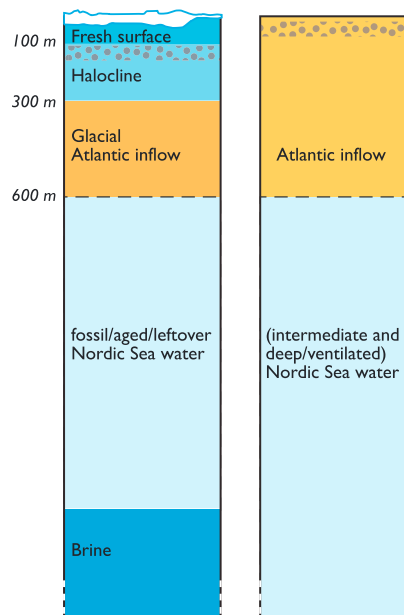


**Figure 4.** A schematic column model of the (left) stadial and (right) interstadial phases consistent with the Nordic sea sediment core MD992284.



the transitions between stadial and interstadial phases and the consistent near-surface temperature trends within the stadial and interstadial periods provide insight into the transition mechanisms and are discussed in section 3.1.

[25] The benthic  $\delta^{18}\text{O}$  record measured on *Cassidulina teretis* (Figure 3d) is remarkably similar to the NGRIP record, exhibiting the characteristic shape and abrupt transitions of D-O cycles. One explanation for the link between the benthic  $\delta^{18}\text{O}$  and NGRIP is provided by *Dokken and Jansen* [1999], who presented evidence that there are two different forms of deep water production in the Nordic seas during the last glacial period, depending on the sea ice coverage. As in the modern climate, there is deep open ocean convection in the Nordic seas during the last glacial period when the surface is free of sea ice. When Greenland is cold (the stadial phase of the D-O cycle), however, they argued that the benthic  $\delta^{18}\text{O}$  becomes lighter in the deep Nordic seas because there is sea ice formation along the Norwegian continental shelf, which creates dense and isotopically light brine water that is subsequently transported down the continental slope and injected into the deeper water. In this scenario, the close link between the benthic  $\delta^{18}\text{O}$  record and NGRIP is due to the deep water being affected by continuous sea ice formation throughout the stadial phase and by open ocean convection during the interstadial phase of the D-O cycle. This interpretation of the benthic record is commensurate with all of the other proxy data in Figure 3, which indicates that during the stadial phase of the D-O cycle, the Nordic seas were covered with sea ice and the surface waters were fresh (Figure 3c) and at the freezing point. Further evidence for the existence of extensive sea ice stems from Figure 3a and modeling work that links the Greenland  $\delta^{18}\text{O}$  record to sea ice extent in the Nordic seas (see section 1).

[26] An alternative interpretation of benthic  $\delta^{18}\text{O}$  at nearby core sites attributes the changes to bottom water temperature rather than brine [*Rasmussen and Thomsen*, 2004]. The temperature change that would be required to explain the 1–1.5‰ shifts seen in benthic  $\delta^{18}\text{O}$  at our site implies a 4–6°C warming at a depth of 1500 m during stadials and almost twice as much during Heinrich events [e.g., *Marcott et al.*, 2011]. We believe that enhanced brine rejection at the surface and moderately increased temperatures at depth act together to create the light benthic  $\delta^{18}\text{O}$  values during stadials and that both processes are necessary for maintaining stadial conditions.

[27] The record of ice-rafted debris (IRD) indicates that there is less frequent ice rafting during cold stadial periods on Greenland (Figure 3e). In this core, the IRD is of Scandinavian origin, and the record implies that there is less calving from the Fennoscandian ice sheet during the cold stadial and therefore less meltwater derived from icebergs. Note that there are two Heinrich events during the time interval shown in Figure 3 (denoted H3 and H4 in Figure 3), both of which occurred during the latter part of a cold stadial phase of a D-O cycle. In this study, we are not concerned with the infrequent, large Heinrich ice rafting events and do not consider Heinrich events to be fundamental to the physics of a D-O cycle. Instead, the reader is referred to the study of *Álvarez-Solas et al.* [2011] for a discussion of the possible relationship between these two phenomena.

[28] In general, the planktonic  $\delta^{13}\text{C}$  exhibits more negative values during stadials (Figure 3f), suggesting that the water at the preferred depth for the planktonic foraminifera is isolated

from the atmosphere. Thus, benthic and planktonic data collectively suggest that during the stadial phase of the D-O cycle, the eastern Nordic seas are characterized by extensive sea ice cover, a surface fresh layer separated by a halocline from warmer, saltier subsurface waters, and by deep water production by brine rejection along the Norwegian coast.

## 2.6. The Nordic Seas During Greenland Interstadials

[29] In the interstadial phase of the D-O cycle, when Greenland is warm (Figure 3a), the Nordic seas are thought to be mostly free of sea ice. Without the presence of sea ice and an associated fresh surface layer, the water column is weakly stratified and the incoming Atlantic water efficiently releases heat to the atmosphere, as is the case in today's Nordic seas (Figure 4, right). As a consequence, subsurface temperatures in the Nordic seas are found to be relatively cold (Figure 3b), and any fresh water that may be deposited in the surface layer is easily removed by strong wind mixing, particularly during the winter.

[30] As shown by *Li et al.* [2005], reduced North Atlantic sea ice cover can account for the warm temperatures observed in the Greenland ice cores during interstadials of the last glacial cycle (Figure 1). Due to the exceptional chronology of the high-resolution marine sediment record, we can confidently link the timing of warm interstadial conditions on Greenland to periods in the marine record with high benthic  $\delta^{18}\text{O}$  (Figure 3d) and well-ventilated conditions in the Nordic seas as evidenced by planktonic  $\delta^{13}\text{C}$  (Figure 3f). The high benthic  $\delta^{18}\text{O}$  values indicate less efficient brine formation combined with lower temperatures, supporting the presence of reduced sea ice cover during interstadials in the Nordic seas [*Dokken and Jansen*, 1999]. Note that the benthic  $\delta^{13}\text{C}$  record (Figure 3g) is not as straightforward to interpret as the planktonic  $\delta^{13}\text{C}$  record: the strong overshoot seen during the transitions between stadial and interstadial conditions is discussed in detail in section 3.2.

## 3. Implications for D-O Cycles

### 3.1. Transition Between Stadial and Interstadial Phases

[31] The records presented thus far support the idea of a reorganization of the vertical thermohaline structure of the Nordic seas between the stadial and interstadial phases of D-O cycles. In the interstadial phase, conditions in the Nordic seas resemble those existing today: the heat transported into the region by the ocean and stored seasonally in the mixed layer is released to the atmosphere, resulting in a moderate, seasonal sea ice cover. In the stadial phase, however, conditions in the Nordic seas resemble those existing in the Arctic Ocean today: there is a fresh surface layer buffered from the warm Atlantic water below by a halocline. In essence, there is an expansion of sea ice southward from the Arctic into the Nordic seas. Indeed, the stratification and vertical structure of the Nordic seas inferred from our proxy data (Figures 3 and 4) are similar to those of today's Arctic, where water is several (~3°C) degrees warmer at a depth of 400–500 m than at the surface in winter [e.g., *Rudels et al.*, 2004].

[32] During the stadial phase, the planktonic foraminifera are mainly recording the temperature of water within, or just below, the halocline (Figure 4, left). The sea ice cover prevents wind mixing, and sea ice formation along the Norwegian coast creates dense brines that are rejected from

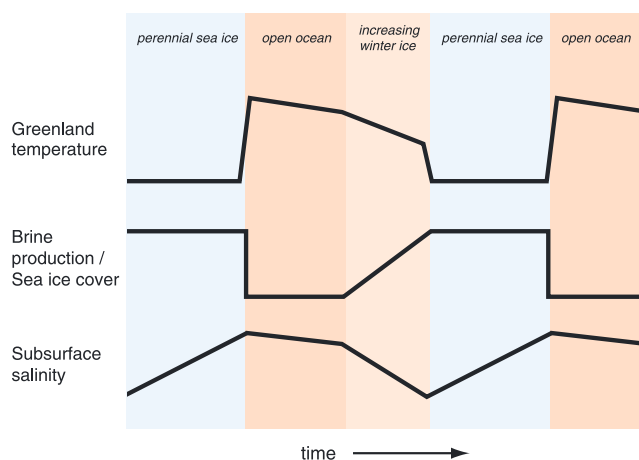


**Figure 5.** A schematic timeline showing the evolution of a D-O cycle that is consistent with the Nordic sea sediment core MD992284 and the NGIP ice core.

the surface and injected deeper in the water column, thus helping to maintain the halocline. As the stadial phase progresses, the planktonic foraminifera show an increase in temperature (Figure 3b) consistent with their depth habitat being continuously fed by the northward advection of relatively warm and salty Atlantic water. With no possibility of venting heat to the atmosphere above, because of extensive sea ice cover, the warming due to the inflow of warm Atlantic water gradually reduces the density of the subsurface waters and weakens the stratification that allows the halocline and sea ice cover to exist. The transition to warm interstadial conditions on Greenland occurs when the stratification and halocline weaken to the point of collapse, at which point heat from the subsurface layer is rapidly mixed up to the surface, melting back the sea ice.

[33] The removal of sea ice in the Nordic seas allows efficient exchange of heat between the ocean and the atmosphere and is seen as an abrupt warming (D-O event) of  $10 \pm 5^\circ\text{C}$  in Greenland at the start of each interstadial [NGRIP, 2004] (Figure 1). There is a distinct overshoot (<100 years long) in foraminifera-derived subsurface temperatures right at the transition (Figure 3b). The planktonic foraminifera live at the interface between the surface and subsurface layers and immediately feel the temperature effect as warm subsurface water is mixed up to the surface. Once the fresh surface layer has been mixed away, the ocean is able to vent heat to the atmosphere. The foraminifera now find themselves living in a new habitat, an *unstratified* surface layer, which is colder than their subsurface stadial habitat.

[34] Once in the interstadial (Figure 4, right), conditions are comparable to those of today: the Nordic seas are relatively ice free, inflowing warm Atlantic water is in contact with the surface, and there is an efficient release of heat to the atmosphere. The planktonic-based temperatures show little change (Figure 3b), but there is a consistent reduction in salinity, in particular, toward the end of each interstadial (Figure 3c). This freshening of the upper part of the Nordic seas water column is most likely due to melting and calving of the nearby Fennoscandian ice sheet in response to the warm climate conditions, as is supported by the increased frequency of IRD deposits at the site toward the end of each interstadial (Figure 3e).

### 3.2. Supporting Evidence From $\delta^{13}\text{C}$

[35] The carbon isotope data from planktonic (*N. Pachyderma* sin.) and benthic (*C. teretis*) foraminifera at the site (Figures 3f and 3g) give additional clues about the transition between stadial and interstadial phases in the Nordic seas. The isotopic signature of carbon ( $\delta^{13}\text{C}$ ) preserved in the calcium carbonate shells of foraminifera is related to ventilation and water mass age: at the surface,  $\text{CO}_2$  exchange with the atmosphere and marine photosynthesis preferentially extract  $^{12}\text{C}$  from seawater, causing enrichment of surface water in dissolved inorganic  $^{13}\text{C}$ . When the water mass is isolated from the surface mixed layer, its  $\delta^{13}\text{C}$  value decreases with age due to mixing with different water masses and gradual decomposition of low  $\delta^{13}\text{C}$  organic matter. Although the benthic foraminifera *C. teretis* do not live directly on the surface of the marine sediments, evidence from studies in the Nordic seas shows that the  $\delta^{13}\text{C}$  of *C. teretis* tracks the  $\delta^{13}\text{C}$  recorded by epibenthic species (benthic fauna living on top of the sediment surface at the seafloor). In the absence of epibenthic foraminifera in high-deposition regions such as the core site, *C. teretis* can be used with caution to infer past changes in deep water  $\delta^{13}\text{C}$  [Jansen et al., 1989].

[36] In the *stadial phase*, with extensive sea ice, relatively young water of Atlantic origin with high  $\delta^{13}\text{C}$  (Figure 3f) enters the Nordic seas below the fresh surface layer and halocline. At the onset of the interstadial, there is a brief period with extremely light benthic  $\delta^{13}\text{C}$  (Figure 3f). This is consistent with a mixing in of old, poorly ventilated deep water masses of Arctic origin from below the Atlantic layer in the Nordic seas [e.g., Thornalley et al., 2011]. Enhanced mixing at the transition will also bring well-ventilated waters with high  $\delta^{13}\text{C}$  down from the surface; however, this signal is overwhelmed by the mixing in of the old water from below with extremely light  $\delta^{13}\text{C}$ .

[37] Early in the *interstadial phase*, following the abrupt transition, the core site is dominated by high  $\delta^{13}\text{C}$  as seen in both the benthic (Figure 3f) and planktonic (Figure 3e) records. At this point, the Nordic seas are free of sea ice and well ventilated, and the stratification is weak due to efficient winter mixing and absence of a halocline. Continuous input of terrestrial freshwater from the Fennoscandian continent also contributes to the high planktonic  $\delta^{13}\text{C}$ . However, toward the end of the interstadial, the influence of sea ice is increasing in the Nordic seas (Figure 3d) and the stratification is increasing, as evidenced by decreasing surface salinity (Figure 3b). As a consequence, benthic  $\delta^{13}\text{C}$  is reduced (Figure 3f), indicating increased stratification and less ventilation of waters at the depth of the core site.

[38] Returning to the stadial phase (Figure 5), with an extensive sea ice cover and return of the halocline, the surface and intermediate waters are now isolated from the atmosphere, as evidenced by relatively low planktonic  $\delta^{13}\text{C}$  values (Figure 3e). Although the qualitative features we have described are robust for each D-O cycle, there are quantitative differences between each cycle. For example, convection may reach deeper during some interstadials than others, making the light spike more pronounced, or the ocean may restratify more quickly during some interstadials, resulting in a more immediate recovery to heavier  $\delta^{13}\text{C}$  values. Such differences will also be reflected in the other proxy records.



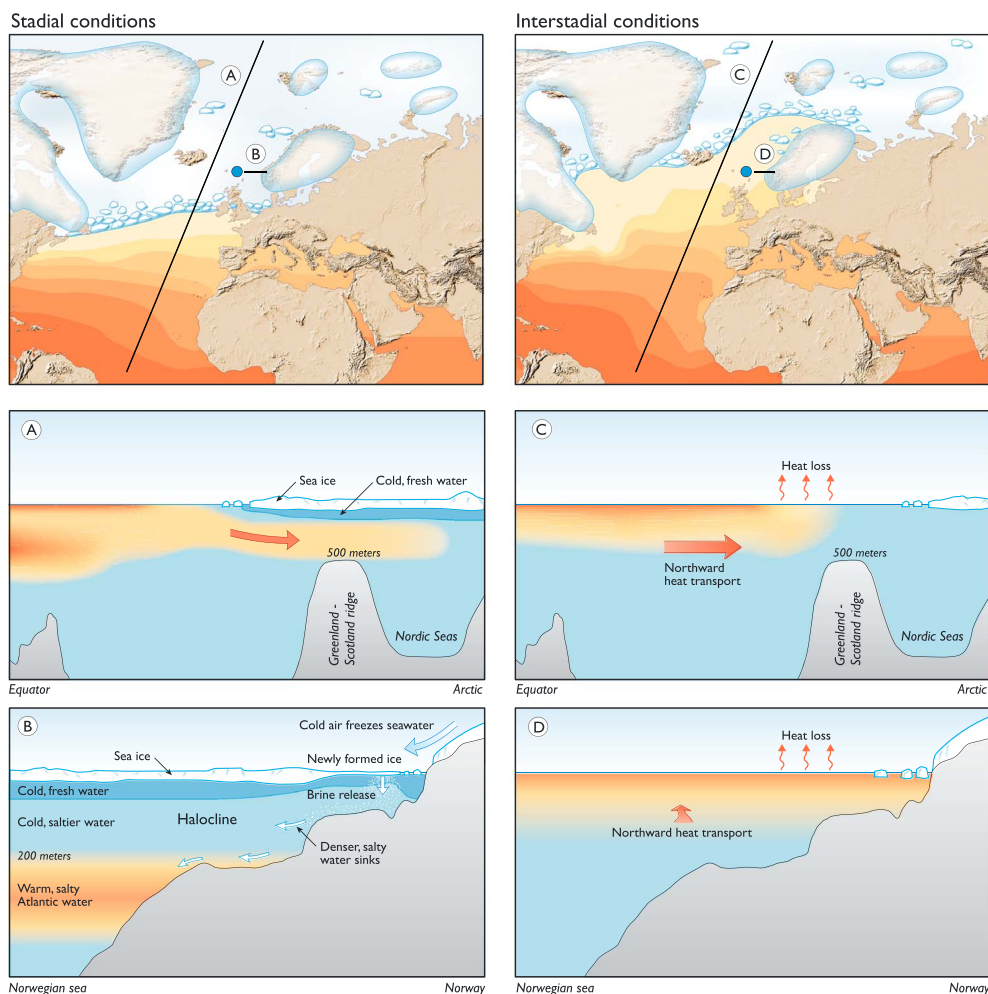


**Figure 6.** Schematic showing wintertime conditions in the North Atlantic and Nordic seas during typical cold stadial periods and (right) warm interstadial periods of a D-O cycle. (top) Maps of the North Atlantic region with sea ice extent and land ice. The location of the sediment core is marked with a blue dot, and the sections described in the bottom panels are indicated. (middle) locations A and C show north-south sections of the North Atlantic during stadial and interstadial conditions, respectively. (bottom) Locations B and D show east-west sections of the Norwegian Sea during stadial and interstadial conditions, respectively.

#### 4. Discussion

[39] The conceptual model for D-O cycles presented in the previous section and summarized in Figures 5 and 6 is based on the proxy records measured in MD992284 and specifically on the relationship between signals in these high-resolution marine records and signals in the Greenland oxygen isotope record. The marine records themselves provide direct information on the water column in the Atlantic inflow region of the Nordic seas. However, the expected changes in sea ice cover illustrated in the conceptual model have implications for the response and role of other parts of the climate system in D-O cycles. We have focused on the Greenland oxygen isotope record as a reference time series for D-O cycles, but additional information is provided by the Greenland deuterium excess record [Jouzel *et al.*, 2005; Masson-Delmotte *et al.*, 2005; Thomas *et al.*, 2009]. Deuterium excess shows a rapid decrease in the temperature of source waters for Greenland precipitation at stadial to interstadial transitions. Assuming that the abrupt transition from stadial to interstadial conditions is

mediated by the removal of sea ice in the Nordic seas, this would provide a new, local source of moisture for precipitation on the Greenland ice sheet during warm interstadials. The ocean temperature of this source would be significantly lower than sources farther to the south [Sachs and Lehman, 1999], thus explaining the observed 3°C rapid decrease in the source temperature for precipitation on Greenland during phases of rapid increase in surface air temperature of D-O cycles [Steffensen *et al.*, 2008].

[40] On a larger scale, changes in sea ice cover are expected to be associated with a reorganization of atmospheric circulation, as is suggested by changes in dust delivered to Greenland [Mayewski *et al.*, 1997]. We hypothesize that during interstadials, the storm track extends northeastward into the Nordic seas, transporting heat into the region and inhibiting formation of sea ice by mechanical mixing. During stadials, the storm track is more zonal and positioned south of the Fennoscandian ice sheet. Experiments with an atmospheric general circulation model forced by various continental ice sheet [Li and Battisti, 2008] and sea ice

configurations [Li *et al.*, 2010] show that a southward displaced jet is also associated with a more quiescent storm track, which would be more conducive to sea ice production in the Nordic seas and with the occurrence of katabatic winds coming off the Fennoscandian ice sheet. In turn, this would promote sea ice production in leads and polynyas on the continental shelf. Shifts in the orientation of the Atlantic storm track could help explain the dust record in Greenland, as well as far-field monsoon and precipitation changes associated with D-O cycles [Pausata *et al.*, 2011].

[41] Many previous models of D-O cycles require, or assume, a flux of freshwater to the North Atlantic mainly from the Laurentide ice sheet in order to maintain extensive sea ice cover over the Nordic seas during stadials. In contrast, the provenance of IRD in MD992284 indicates that the freshwater forcing originates from the Fennoscandian ice sheet and is associated with interstadials as much as, if not more than, stadials. This provides a local freshwater source in the path of the Atlantic inflow in a highly sensitive area of the Nordic seas, which can aid more directly in creating a halocline and facilitating expansion of sea ice compared to freshwater sources on the western rim of the North Atlantic.

[42] We further expect that the presence of a halocline and extensive sea ice during stadials greatly reduces the ventilation of the deep ocean as it prevents contact between inflowing Atlantic water and the atmosphere in the Nordic seas. This will impact the properties of the return flow of Atlantic water leaving the Nordic seas and should be recorded by intermediate and deepwater proxies throughout MIS3. The marine proxy data presented in this study support the existence of an active circulation of relatively warm Atlantic water into the Nordic seas during stadials but do not give a direct measure of the rate of Atlantic meridional overturning circulation. Evaluating changes in the AMOC as a response to enhanced stratification in the Nordic seas during stadials is beyond the scope of this study. However, such changes are expected, as the returning outflow of Atlantic water from the Nordic seas would not be sufficiently dense to sink into the deep abyss during stadials. As discussed in several studies [Crowley, 1992; Stocker and Johnsen, 2003], a reduction in the AMOC could lead to warming of the Southern Ocean and possibly explain the “see-saw” pattern with warm temperatures on Antarctica when Greenland is cold [EPICA, 2006; Blunier and Brook, 2001].

[43] MIS3 records from other Nordic seas marine cores share many consistent features with the records presented in this study. However, different interpretations of these features lead to hypothesized mechanisms for D-O cycles that are different from ours in important ways. For example, Rasmussen and Thomsen [2004] suggest that there is warming at depth during stadials, based on the depleted benthic  $\delta^{18}\text{O}$  from a sediment core obtained from the central Nordic seas basin at 1000 m depth. We also observe depleted benthic  $\delta^{18}\text{O}$  during stadials at our core site, but we interpret this primarily to be due to brine production. Given the position of our core on the Norwegian slope, interpreting the depleted benthic  $\delta^{18}\text{O}$  exclusively as a temperature signal would imply temperatures of 4–6°C warmer during stadial periods at a depth of 1500 m in the Nordic seas, which we find unlikely.

[44] Another example, Petersen *et al.* [2013] hypothesize that the duration of the interstadial and stadial phases of the D-O cycles is related to ice shelves, while sea ice changes

provide the abrupt transitions. Critical support for this ice shelf mechanism is an increase in ice rafting during each D-O stadial inferred from IRD and fresh surface anomalies based on planktonic  $\delta^{18}\text{O}$  [Dokken and Jansen, 1999; van Kreveld *et al.*, 2000; Elliot *et al.*, 1998, 2001]. The postulated occurrence of ice rafting during cold Greenland stadials, as required by the Petersen *et al.* [2013] hypothesis, appears to disagree with the chronology of our marine sediment core, in which ice rafting is enhanced during the latter part of the interstadials (Figure 3e). However, Petersen *et al.* [2013] focus on the Irminger Basin, which is far enough away from our core site that there may be no inconsistency. Note also that in the earlier studies, using cores with a lower sedimentation rate, there is hardly any sedimentation during stadials, leaving nearly only coarse-grained lithic content. This could indicate that the fraction of coarse- to fine-grained sediment is not solely due to changes in iceberg calving, but could partly be due to reduced sedimentation rates and runoff during the cold stadial periods when the Nordic seas are thought to be covered by extensive sea ice.

[45] In accordance with our model for the D-O cycles, the warm interstadials, with reduced sea ice cover and enhanced precipitation over Fennoscandia, will cause the ice sheet to grow, resulting in increased calving and enhanced IRD (Figure 3e) toward the end of the interstadial, lasting partly into the following stadial. The presence of extensive sea ice during the cold stadial will decrease precipitation on the ice sheet and gradually reduce the calving and runoff from Fennoscandia, as seen in the decreased occurrence of IRD.

[46] Ultimately, our hypothesized reorganization of the Nordic seas circulation during D-O cycles is not dependent on the input of meltwater from melting ice sheets. However, these issues show that open questions remain, requiring better spatial coverage of marine sediment cores with adequate chronology to pin down the correct timing of reconstructed oceanic signals compared to the ice core records.

[47] Our conceptual model of D-O cycles requires the presence of a shallow ocean over a continental shelf adjacent to the Fennoscandian ice sheet. Should the Fennoscandian ice sheet extend over the continental shelf, the stadial phase of the proposed D-O cycle could not exist because brine production through sea ice formation would not be possible, and thus, a stable halocline could not be maintained in the Nordic seas. Hence, consistent with observations, our conceptual model precludes the possibility of D-O cycles at the Last Glacial Maximum, when the Fennoscandian ice margin was located near the shelf break. Furthermore, with less efficient brine production at the Last Glacial Maximum, we expect that sea ice formation will be reduced compared to a typical stadial, resulting in ice-free conditions over large parts of the Nordic seas [Hebbeln *et al.*, 1994].

[48] Finally, we can draw an analogy between the stadial phase in the Nordic seas during the last glacial period and the Arctic Ocean today. Both feature a fresh surface layer, halocline, and extensive sea ice. The existence of these features is sensitive to the heat transported by inflowing Atlantic water and to brine release during sea ice formation on the continental shelves. Projections of global warming [Holland and Bitz, 2003] are consistent with observed trends [Smedsrud *et al.*, 2008] showing increased heat transport to the Arctic Ocean by the Atlantic inflow. Together with reduced sea ice formation, this will weaken the halocline

and could rapidly tip the Arctic Ocean into a perennially ice-free phase. In such a phase, warm Atlantic water will be brought to the surface and have a severe impact on Arctic climate and the stability of the Greenland ice sheet.

[49] **Acknowledgments.** We gratefully acknowledge Carin Andersson Dahl for calculating the foram-based temperatures and wish to thank the IMAGES program and the R/V *Marion Dufresne* crew on leg MD114. Our work greatly benefited from discussions with Øyvind Lie, Andrey Ganopolski, Jorge-Alvarez-Solas, Gilles Ramstein, Juliette Mignot, Hans Renssen, Frank Peeters Ben Marzeion, and Tor Eldevik, as well as reviews of an early version of the manuscript by Eystein Jansen and Ulysses Ninnemann, and three anonymous referees. This work was supported by the VAMOC project funded by the Norwegian Research Council and is publication A429 from the Bjerknes Centre for Climate Research.

## References

- Álvarez-Solas, J., M. Montoya, C. Ritz, G. Ramstein, S. Charbit, C. Dumas, K. Nisancioglu, T. Dokken, and A. Ganopolski (2011), Heinrich event 1: An example of dynamical ice-sheet reaction to oceanic changes, *Clim. Past, Copernicus Publications*, 7, 1297–1306.
- Bigg, G. R., and E. J. Rohling (2000), An oxygen isotope data set for marine waters, *J. Geophys. Res.*, 105, 8527–8536.
- Birchfield, G. E., and W. S. Broecker (1990), A salt oscillator in the glacial ocean? Part II: A 'scale analysis' model, *Paleoceanography*, 5, 835–843.
- Blunier, T., and E. J. Brook (2001), Timing of millennial-scale climate change in Antarctica and Greenland during the last glacial period, *Science*, 291, 109–112.
- Bond, G., W. Broecker, S. Johnsen, J. McManus, L. Labeyrie, J. Jouzel, and G. Bonani (1993), Correlations between climate records from North Atlantic sediments and Greenland ice, *Nature*, 365, 143–147.
- Broecker, W. (2000), Abrupt climate change: Causal constraints provided by the paleoclimate record, *Earth-Science Reviews*, 51, 137–154.
- Broecker, W. S., D. M. Peteet, and D. Rind (1985), Does the ocean–atmosphere system have more than one stable mode of operation, *Nature*, 315, 21–26.
- Broecker, W. S., G. Bond, and M. Klas (1990), A salt oscillation in the glacial Atlantic? 1. The concept, *Paleoceanography*, 5, 469–477.
- Carstens, J., D. Hebbeln, and G. Wefer (1997), Distribution of planktic foraminifera at the ice margin in the Arctic (Fram Strait), *Marine Micropaleontology*, 29, 257–269.
- Chiang, J. C. H., M. Biasutti, and D. S. Battisti (2003), Sensitivity of the Atlantic Intertropical Convergence Zone to Last Glacial Maximum boundary conditions, *Paleoceanography*, 18(4), 1094, doi:10.1029/2003PA000916.
- Clark, P. U., S. J. Marshall, G. K. C. Clarke, S. W. Hostetler, J. M. Licciardi, and J. T. Teller (2001), Freshwater forcing of abrupt climate change during the last glaciation, *Science*, 293, 283–287.
- Crowley, T. J. (1992), North Atlantic deep water cools the Southern Hemisphere, *Paleoceanography*, 7, 489–497.
- Curry, W. B., and D. W. Oppo (1997), Synchronous, high-frequency oscillations in tropical sea surface temperatures and North Atlantic Deep Water production during the last glacial cycle, *Paleoceanography*, 12, 1–14.
- Dansgaard, W., et al. (1993), Evidence for general instability of past climate from a 250-kyr ice core record, *Nature*, 364, 218–220.
- Davies, S. M., S. Wastegård, T. L. Rasmussen, A. Svensson, S. J. Johnsen, J. P. Steffensen, and K. K. Andersen (2008), Identification of the Fugloyarbanki tephra in the NGRIP ice core: A key tie point for marine and ice-core sequences during the last glacial period, *Journ. of Quaternary Science*, 23, 409–414.
- Dokken, T. M., and E. Jansen (1999), Rapid changes in the mechanism of ocean convection during the last glacial period, *Nature*, 401, 458–461.
- Elliot, M., L. Labeyrie, G. Bond, E. Cortijo, J.-L. Turon, N. Tisnerat, and J.-C. Duplessy (1998), Millennial-scale iceberg discharges in the Irminger Basin during the last glacial period: Relationship with the Heinrich events and environmental settings, *Paleoceanography*, 13, 433–446.
- Elliot, M., L. Labeyrie, T. Dokken, and S. Manthe (2001), Coherent patterns of ice-rafted debris deposits in the Nordic regions during the last glacial (10–60 ka), *Earth Planet. Sci. Lett.*, 194, 151–163.
- EPICA community members (2006), One-to-one coupling of glacial climate variability in Greenland and Antarctica, *Nature*, 444, 195–198.
- Fairbanks, R. G. (1989), A 17,000-year glacio-eustatic sea-level record: Influence of glacial melting rates on the Younger Dryas event and deep-ocean circulation, *Nature*, 342, 637–642.
- Fairbanks, R. G., R. A. Mortlock, T. C. Chiu, L. Cao, A. Kaplan, T. P. Guilderson, T. W. Fairbanks, A. L. Bloom, P. M. Grootes, and M. J. Nadeau (2005), Radiocarbon calibration curve spanning 0 to 50,000 years BP based on paired Th-230/U-234/U-238 and C-14 dates on pristine corals, *Quaternary Science Reviews*, 24, 1781–1796.
- Ganopolski, A., and S. Rahmstorf (2001), Rapid changes of glacial climate simulated in a coupled climate model, *Nature*, 409, 153–158.
- Genty, D., D. Blamart, R. Ouahdi, M. Gilmour, A. Baker, J. Jouzel, and S. Van-Exter (2003), Precise dating of Dansgaard-Oeschger climate oscillations in western Europe from stalagmite data, *Nature*, 421, 833–837.
- Gildor, H., and E. Tziperman (2003), Sea-ice switches and abrupt climate change, *Phil. Trans. R. Soc. Lond. A*, 361, 1935–1942, doi:10.1098/rsta.2003.1244.
- Hebbeln, D., T. Dokken, E. S. Andersen, M. Hald, and A. Elverhoi (1994), Moisture supply for northern ice-sheet growth during the Last Glacial Maximum, *Nature*, 370, 357–360.
- Hendy, I. L., J. P. Kennett, E. B. Roark, and B. L. Ingram (2002), Apparent synchronicity of submillennial scale climate events between Greenland and Santa Barbara Basin, California from 30–10 ka, *Quaternary Science Reviews*, 21, 1167–1184.
- Holland, M. M., and C. M. Bitz (2003), Polar amplification of climate change in coupled models, *Clim. Dyn.*, 21, 221–232.
- Huber, C., M. Leuenberger, R. Spahni, J. Flückiger, J. Schwander, T. F. Stocker, S. Johnsen, A. Landais, and J. Jouzel (2006), Isotope calibrated Greenland temperature record over Marine Isotope Stage 3 and its relation to CH<sub>4</sub>, *Earth Planet. Sci. Lett.*, 243, 504–519.
- Hughen, K. A., et al. (2004), Marine04 marine radiocarbon age calibration, 0–26 ka BP, *Radiocarbon*, 46, 1059–1086.
- Jansen, E., B. Slettemark, U. Bleil, R. Henrich, L. Kringstad, and S. Rolfsen (1989), Oxygen and carbon isotope stratigraphy and magnetostratigraphy of the last 2.8 Ma: Paleoclimatic comparisons between the Norwegian Sea and the North Atlantic, *Proceedings of the Ocean Drilling Program Scientific Results*, 104, 255–269.
- Jouzel, J., V. Masson-Delmotte, M. Stievenard, A. Landais, F. Vimeux, S. J. Johnsen, A. E. Sveinbjornsdottir, and J. W. White (2005), Rapid deuterium-excess changes in Greenland ice cores: A link between the ocean and the atmosphere, *C.R. Geosci.*, 337, 957–969.
- Kim, S.-T., and J. R. O'Neil (1997), Equilibrium and nonequilibrium oxygen isotope effects in synthetic carbonates, *Geochim. Cosmochim. Acta*, 61, 3461–3475.
- Kissel, C., C. Laj, L. Labeyrie, T. Dokken, A. Voelker, and D. Blamart (1999), Rapid climatic variations during marine isotope stage 3: Magnetic analysis of sediments from Nordic Seas and North Atlantic, *Earth Planet. Sci. Lett.*, 171, 489–502.
- Knutti, R., J. Flückiger, T. Stocker, and A. Timmermann (2004), Strong hemispheric coupling of glacial climate through freshwater discharge and ocean circulation, *Nature*, 430, 851–856.
- Landais, A., N. Caillon, J. Severinghaus, J. M. Barnola, C. Goujon, J. Jouzel, and V. Masson-Delmotte (2004), Isotopic measurements of air trapped in ice to quantify temperature changes, *C.R. Geosci.*, 336, 963–970.
- Lang, C., M. Leuenberger, J. Schwander, and S. Johnsen (1999), 16°C rapid temperature variation in Central Greenland 70,000 years ago, *Science*, 286, 934–937.
- Lewis, S. C., A. N. LeGrande, M. Kelley, and G. A. Schmidt (2010), Water vapour source impacts on oxygen isotope variability in tropical precipitation during Heinrich events, *Clim. Past*, 6, 325–343.
- Li, C., and D. S. Battisti (2008), Reduced Atlantic storminess during last glacial maximum: Evidence from a coupled climate model, *J. Climate*, 21, 3561–3579.
- Li, C., D. S. Battisti, D. P. Schrag, and E. Tziperman (2005), Abrupt climate shifts in Greenland due to displacements of the sea ice edge, *Geophys. Res. Lett.*, 32, L19702, doi:10.1029/2005GL023492.
- Li, C., D. S. Battisti, and C. M. Bitz (2010), Can North Atlantic sea ice anomalies account for Dansgaard-Oeschger climate signals?, *J. Climate*, 23, 5457–5475.
- Manabe, S., and R. J. Stouffer (1988), Two stable equilibria of a coupled ocean–atmosphere model, *J. Climate*, 1, 841–866.
- Marcott, S. A., et al. (2011), Ice-shelf collapse from subsurface warming as a trigger for Heinrich events, *Proc. Nat. Acad. Sci.*, 108, 13,415–13,419.
- Marotzke, J., and J. Willebrand (1991), Multiple equilibria of the global thermohaline circulation, *J. Phys. Oceanogr.*, 21, 1372–1385.
- Masson-Delmotte, V., J. Jouzel, A. Landais, M. Stievenard, S. J. Johnsen, J. W. C. White, M. Werner, A. Sveinbjornsdottir, and K. Fuhrer (2005), GRIP deuterium excess reveals rapid and orbital-scale changes in Greenland moisture origin, *Science*, 309, 118–121.
- Mayewski, P. A., L. D. Meeker, M. S. Twickler, S. I. Whitlow, Q. Yang, W. B. Lyons, and M. Prentice (1997), Major features and forcing of high latitude northern hemisphere atmospheric circulation over the last 110,000 years, *J. Geophys. Res.*, 102, 26,345–26,366.
- Meland, M. Y., E. Jansen, and H. Elderfield (2005), Constraints on SST estimates for the northern North Atlantic Nordic seas during the LGM, *Quat. Sci. Rev.*, 24, 835–852.

- Mignot, J., A. Ganopolski, and A. Levermann (2007), Atlantic subsurface temperatures: Response to a shutdown of the overturning circulation and consequences for its recovery, *J. Climate*, *20*, 4884–4898.
- North Greenland Ice Core Project members (2004), High-resolution record of Northern Hemisphere climate extending into the last interglacial period, *Nature*, *431*, 147–151.
- Otto-Bliesner, B. L., and E. C. Brady (2010), The sensitivity of the climate response to the magnitude and location of freshwater forcing: Last glacial maximum experiments, *Quat. Sci. Rev.*, *29*, 56–73.
- Paillard, D. L., L. Labeyrie, and P. Yiou (1996), Macintosh program performs time-series analysis, *EOS Transactions AGU*, *77*, 379.
- Pausata, F. S. R., D. S. Battisti, K. H. Nisancioglu, and C. M. Bitz (2011), Chinese stalagmite  $\delta^{18}\text{O}$  controlled by changes in the Indian monsoon during a simulated Heinrich event, *Nat. Geosci.*, *4*, 474–480.
- Petersen, S. V., D. P. Schrag, and P. Clark (2013), A new mechanism for Dansgaard-Oeschger cycles, *Paleoceanography*, *28*, 24–30, doi:10.1029/2012PA002364.
- Peterson, L. C., G. H. Haug, K. A. Hughen, and U. Rohl (2000), Rapid changes in the hydrologic cycle of the tropical Atlantic during the last glacial, *Science*, *290*, 1947–1951.
- Pflaumann, U., et al. (2003), Glacial North Atlantic: Sea-surface conditions reconstructed by GLAMAP 2000, *Paleoceanography*, *18*(3), 1065, doi:10.1029/2002PA000774.
- Rahmstorf, S. (2002), Ocean circulation and climate during the past 120,000 years, *Nature*, *419*, 207–214.
- Rasmussen, T. L., and E. Thomsen (2004), The role of the North Atlantic Drift in the millennial timescale glacial climate fluctuations, *Palaeogeogr. Palaeoclimatol. Palaeoecol.*, *210*, 101–116.
- Renssen, H., and R. Isarin (2001), The two major warming phases of the last deglaciation at ~14.7 and ~11.5 ka cal BP in Europe: Climate reconstructions and AGCM experiments, *Global Planet. Change*, *30*, 117–153.
- Rudels, B., E. P. Jones, U. Schauer, and P. Eriksson (2004), Atlantic sources of the Arctic Ocean surface and halocline waters, *Polar Research*, *23*, 181–208.
- Sachs, J. P., and S. J. Lehman (1999), Subtropical North Atlantic temperatures 60,000 to 30,000 years ago, *Science*, *286*, 756–759.
- Schulz, H., U. von Rad, and H. Erlenkeuser (1998), Correlation between Arabian Sea and Greenland climate oscillations of the past 110,000 years, *Nature*, *393*, 54–57.
- Severinghaus, J. P., and E. J. Brook (1999), Abrupt climate change at the end of the last glacial period inferred from trapped air in polar ice, *Science*, *286*, 930–934.
- Siddall, M., E. J. Rohling, W. G. Thompson, and C. Waelbroeck (2008), Marine isotope stage 3 sea level fluctuations: Data synthesis and new outlook, *Rev. Geophys.* *46*, RG4003, doi:10.1029/2007RG000226.
- Smedsrud, L. H., A. Sorteberg, and K. Kloster (2008), Recent and future changes of the Arctic sea-ice cover, *Geophys. Res. Lett.*, *35*, L20503, doi:10.1029/2008GL034813.
- Steffensen, J. P., et al. (2008), High-resolution Greenland ice core data show abrupt climate change happens in few years, *Science*, *321*, 680–684.
- Stocker, T. F., and S. J. Johnsen (2003), A minimum thermodynamic model for the bipolar seesaw, *Paleoceanography*, *18*(4), 1087, doi:10.1029/2003PA000920.
- Stommel, H. (1961), Thermohaline convection with two stable regimes of flow, *Tellus*, *13*, 224–230.
- Stuiver, M., and P. J. Reimer (1993), Extended C database and revised CALIB 3.0 14C age calibration program, *Radiocarbon*, *35*, 215–230.
- Svensson, A., et al. (2006), The Greenland Ice Core Chronology, 2005, 15–42 ka. Part 2: Comparison to other records, *Quat. Sci. Rev.*, *25*, 3258–3266.
- Svensson, A., et al. (2008), A 60 000 year Greenland stratigraphic ice core chronology, *Climate Of The Past*, *4*, 47–57.
- Telford, R. J., and H. J. B. Birks (2005), The secret assumption of transfer functions: Problems with spatial autocorrelation in evaluating model performance, *Quat. Sci. Rev.*, *24*, 2173–2179.
- Thomas, E. R., E. W. Wolff, R. Mulvaney, S. J. Johnsen, J. P. Steffensen, C. Arrowsmith (2009), Anatomy of a Dansgaard-Oeschger warming transition: High resolution analysis of the North Greenland Ice Core Project ice core, *J. Geophys. Res.*, *114*, D08102, doi:10.1029/2008JD011215.
- Thornalley, D. J. R., S. Barker, W. S. Broecker, H. Elderfield, and I. N. McCave (2011), The deglacial evolution of North Atlantic deep convection, *Science*, *331*, 202–205.
- van Kreveld, S., M. Sarnthein, H. Erlenkeuser, P. Grootes, S. Jung, M. J. Nadeau, U. Pflaumann, and A. Voelker (2000), Potential links between surging ice sheets, circulation changes, and the Dansgaard-Oeschger cycles in the Irminger Sea, 60–18 kyr RID B-5084-2010, *Paleoceanography*, *15*, 425–442.
- Vellinga, M., and R. A. Wood (2002), Global climatic impacts of a collapse of the Atlantic thermohaline circulation, *Clim. Change*, *54*, 251–267.
- Voelker, A. H. L. (2002), Global distribution of centennial-scale records for Marine Isotope Stage (MIS) 3: A database, *Quat. Sci. Rev.*, *21*, 1185–1212.
- Waelbroeck, C., L. Labeyrie, E. Michel, J. C. Duplessy, J. F. McManus, K. Lambeck, E. Balbon, and M. Labracherie (2002), Sea level and deep water temperature changes derived from benthonic foraminifera isotopic records, *Quat. Sci. Rev.*, *21*, 295–305.
- Wagner, J. D. M., J. E. Cole, J. W. Beck, P. J. Patchett, G. M. Henderson, and H. R. Barnett (2010), Moisture variability in the southwestern United States linked to abrupt glacial climate change, *Nat. Geosci.*, *3*, 110–113.
- Wastegård, S., T. L. Rasmussen, A. Kuijpers, T. Nielsen, and T. C. E. van Weering (2006), Composition and origin of ash zones from Marine Isotope Stages 3 and 2 in the North Atlantic, *Quat. Sci. Rev.*, *25*, 2409–2419.

## **Author's Note**

We would like to clarify further the similarities and differences between our conclusions and prior research. Our manuscript provided a model for Dansgaard-Oeschger cycles in which brine rejection along the Norwegian coast is critical for the development of the cycles. Our data and the interpretation of it is different from the standard model of Dansgaard-Oeschger cycles (which is after Broecker et al., 1985 and what is described in Rasmussen and Thomsen, 2004). Indeed, important parts of the standard model are incompatible with our data and interpretation. For example, the standard model requires cyclic freshwater forcing from the ice sheets, but our data suggest that the ice sheet passively responded to the climate changes associated with Dansgaard-Oeschger cycles and that brine rejection along the Norwegian coast acted to (i) re-stabilize the Nordic Seas and (ii) initiate the transition from interstadial to stadial state in the cycle. This aspect was not clear in the related Eos highlight, and our text, diagrams, and references could have clarified the similarities and differences with previous work in greater depth, and the reader is thus alerted to examine these.